Cellulose (2011) 18:1599–1609
DOI 10.1007/s10570-011-9579-y

Preparation and characterization of hydrophobic derivatives of TEMPO-oxidized nanocelluloses

Richard K. Johnson · Audrey Zink-Sharp · Wolfgang G. Glasser

Received: 4 May 2011 / Accepted: 25 July 2011 / Published online: 10 August 2011

Abstract Amidation and ionic complexation were evaluated as surface modification treatments for TEMPO-oxidized nanocelluloses (TONc), using octadecylamine (ODA) as the modifying compound. Effects of the two treatments on TONc with respect to degree of ODA substitution, surface hydrophobicity, crystalline characteristics, and thermal decomposition properties were investigated, respectively, with elemental analysis, contact angle measurements, X-ray diffraction spectroscopy, and thermogravimetric analysis. Both treatments resulted in complete substitution of TONc surface carboxyl groups with ODA, transforming TONc surfaces from hydrophilic to hydrophobic. A slightly greater than one-to-one ODA-to-carboxyl ratio was found for the ionic complexation product, giving it a more hydrophobic character than the amidation product. Furthermore, the ionic complexation product was found to be surprisingly stable in acidic environment and was able to resist dissociation at fairly low pH. TONc from both treatments could be readily dispersed in organic solvents of wide-ranging polarities, making ionic complexation an equally effective surface modification approach as amidation for the hydrophobization of TONc surfaces. It was also found, through X-ray diffraction results that the crystalline structure of TONc was preserved even after the surface modification treatments. Finally, the thermal stability of TONc was slightly increased as a result of the surface modification treatments as evidenced by slight shifts to higher values of TONc thermal decomposition temperature.

Keywords TEMPO · Nanocellulose · Surface modification · Octadecylamine · Amidation · Ionic complexation

Introduction

Preparation of individualized, surface-carboxylated nanocelluloses was recently reported (Saito et al. 2006a, 2007). This new class of nanocelluloses was derived from the mechanical disintegration of TEMPO-oxidized cellulose fibers, and is referred to in the present study as TEMPO-oxidized nanocelluloses (TONc). TONc have been employed as components in a variety of patented applications namely oxygen barrier (Mukai et al. 2010), gel (Isogai et al. 2010b), thickener (Isogai et al. 2010c), papermaking (Suzuki et al. 2009), composite (Kato et al. 2010), and cosmetic (Isogai et al. 2010a) preparations. Another potential application of TONc that has not yet been explored is their use in non-aqueous

Electronic supplementary material The online version of this article (doi:10.1007/s10570-011-9579-y) contains supplementary material, which is available to authorized users.

R. K. Johnson · A. Zink-Sharp (✉) · W. G. Glasser
Department of Wood Science and Forest Products, Virginia Polytechnic Institute and State University, 230 Cheatham Hall, Blacksburg, VA 24061-0323, USA
e-mail: agzink@vt.edu

media-based applications such as reinforcing additives in water-insoluble polymers. Many of the reported attributes of TONc (high fibril individualization leading to aqueous suspension transparency, very small (3–5 nm) fibril widths, and retention of the crystallinity of native cellulose (Saito and Isogai 2004; Saito et al. 2005, 2006b; Habibi et al. 2006)) could be favorable for their performance as reinforcing additives in polymer nanocomposites. However, the high concentration of surface carboxyl groups makes TEMPO-oxidized celluloses, in general, strongly hydrophilic, with water retention values of 400 and 200% for the salt and free acid forms respectively (Saito et al. 2007). Irrespective of their potential appeal as bio-based reinforcing additives, TONc have thus far been explored only in water-based polymeric systems such as hydroxypropylcellulose and polyphenol (Johnson et al. 2009; Li et al. 2010).

In past studies, hydrophobization of TONc has been targeted at their surface carboxyl groups through carbodiimide-mediated coupling to amine-functionalized molecules (Araki et al. 2001; Zhu et al. 2001; Follain et al. 2008, 2010; Lasseuguette 2008; Azzam et al. 2010). For example, the work of Araki et al. (2001) involved coupling of amine-terminated polyethylene glycol (PEG-NH_2) chains onto the surfaces of TEMPO-oxidized cellulose whiskers. Amidation was achieved with the use of 1-ethyl-3-(3-dimethylaminopropyl) carbodiimide (EDC) (Fig. 1a), in combination with N-hydroxysuccinimide (NHS) (Fig. 1b) as coupling agents. In related studies, EDC/NHS-mediated amidation was employed to couple amine-functionalized entities to cotton, wood, and sugar beet pulp-derived TONc (Lasseuguette 2008; Follain et al. 2010). TEMPO-mediated oxidation also results in partial functionalization of cellulose fiber surfaces with aldehyde groups (Saito et al. 2006a). In their study involving EDC-mediated amidation of

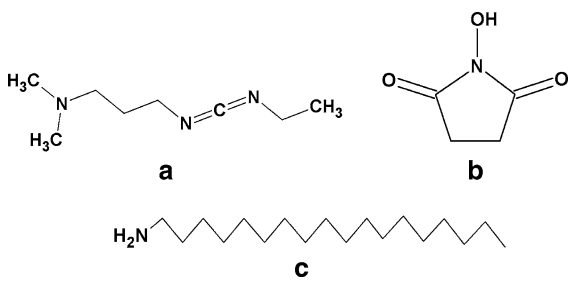

Fig. 1 Structures of **a** EDC, **b** NHS, and **c** octadecylamine

thermosensitive polyetheramines onto TEMPO-oxidized nanocelluloses, Azzam et al. (2010) observed a ^{13}C-NMR signal at 155 ppm, which they attributed to the likely formation of imine bonds between polyetheramines and aldehyde groups on the nanocellulose surfaces. Surface modification of TONc has not only been limited to covalent coupling reactions but has also been accomplished by non-covalent adsorption of hydrophobic molecules onto TONc carboxyl sites. Fukuzumi et al. (2009) demonstrated the non-covalent adsorption of alkylketene dimer (AKD) onto the carboxylate sites of TONc films. Exposure of the TONc films to an AKD solution (0.05%) for 10 s increased the water contact angle on the film surfaces from 47 to 94°.

In this study, we employed both amidation and ionic complexation (electrostatic adsorption) as treatment techniques for the attachment of octadecylamine (ODA, Fig. 1c) to the surfaces of TONc. ODA was selected for its water insolubility and strong hydrophobicity. Our goal was to study the effects of the two treatment techniques on the degree of ODA substitution, surface polarity, crystalline characteristics, and thermal decomposition properties of TONc. Miscibility between aqueous TONc suspensions and ODA was achieved with a water-dimethylformamide (DMF) co-solvent system.

Experimental

Materials

Never-dried pulp (Douglas-fir), derived from the kraft process, was kindly donated by Weyerhaeuser Company, Longview, WA. TEMPO (99.8%), sodium hypochlorite (NaOCl) solution (reagent grade, 13.4% available chlorine), sodium bromide (NaBr, 99.0%), NaOH and HCl standard solutions, ethanol (200 proof), octadecylamine (ODA, 99.0%), and DMF (ACS reagent grade, 99.8%) were purchased from Sigma-Aldrich. EDC and NHS (>98.0% purity) were purchased from Pierce Protein Research, Rockford, IL.

Preparation of TONc

Never-dried pulp for the preparation of TONc was TEMPO-oxidized in accordance with previous reports (Saito et al. 2007; Johnson et al. 2009). To

obtain TONc, the oxidized pulp suspensions (0.5 wt% in ultrapure water) were sonicated in 150 mL batches with an ultrasonic processor (Sonics and Materials VC 750). Sonication was performed for 20 min in a double-walled glass cooling cell connected to a cooling bath, to prevent overheating of the pulp suspensions. Unfibrillated and partially fibrillated pulp were removed by centrifugation (Eppendorf Centrifuge Model 5804, 5 min, 4,500 rpm). The transparent TONc suspensions were acidified to pH < 1.5 (using 1.0 N HCl) to convert TONc carboxylates to their acid form. The suspensions were then dialyzed (Spectra/Por regenerated cellulose membranes, Spectrum Laboratories, cut-off molecular weight 12–14 kD) to pH $\sim$4.5 and kept refrigerated (5–8 °C) until used.

Surface modification of TONc

To achieve miscibility between ODA and aqueous TONc suspensions, a 4% w/v ODA solution was prepared in DMF and then mixed with the TONc suspensions. For both ionic complexation and amidation treatments, an ODA-to-TONc carboxyl ratio of 4:1 was used. First, the TONc suspensions (1,000 mL of 0.5 wt%, 8.1 mmol COOH) were prepared in three-neck flasks with overhead stirring (400–500 rpm) and equilibrated in an oil bath at 50 °C. With respect to ionic complexation, the ODA (8.7 g (32.4 mmol) in 250 mL DMF)-TONc mixture was maintained at pH 7.5–8.0 (using 0.5 N NaOH or 1 N HCl) for 4 h. The amidation treatment followed the EDC/NHS-mediated coupling procedure used in previous studies (Araki et al. 2001; Follain et al. 2008; Lasseuguette 2008) with minor modifications. First, EDC (7.76 g, 40.5 mmol) and NHS (5.59 g, 48.6 mmol) were dissolved in ultrapure water (20 mL) and added to the preconditioned TONc suspension. pH of the mixture was adjusted to and maintained at 5.5–6.0 for 30 min to allow TONc surface activation and then the ODA solution was added. The pH was readjusted to 7.5–8.0 and the reaction was allowed to proceed for 12 h. A control sample was also prepared by subjecting a TONc suspension to the treatment conditions but with the exclusion of ODA or coupling agents. The products of ionic complexation and amidation were designated *ICmplx* and *Amd* respectively. Figure 2 is a reaction scheme summarizing the two surface modification treatments.

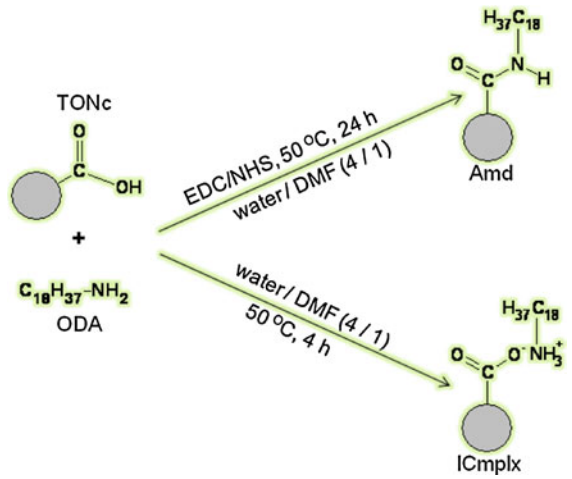

Fig. 2 Simplified schemes for modification of TONc surfaces to Amd and ICmplx

The treated samples were recovered by centrifugation, dialysis, and freeze-drying. First, centrifugation was used to isolate the nanocelluloses from the reaction medium. The nanocellulose residues were twice dispersed in ultrapure water and centrifuged to remove residual reagents. Subsequent water washes, to neutral pH, were interrupted with HCl (0.1 N) and ethanol washes to, respectively, regenerate any unconverted carboxyls remaining and to extract any unbound ODA after the treatments. The washed nanocelluloses were then dialyzed as already described (see section on TONc preparation) and dialysis was ended when the conductivity of the surrounding water remained constant.

Preparation of test samples

Fractions of dialyzed suspensions were refrigerated (5–8 °C), freeze-dried, or solvent-cast from 80% ethanol solutions into films (200 $\pm$ 40 μm thick by solvent evaporation in a fume hood). Freeze-dried samples and films were further dried in vacuum (1.33 mbar, 50 °C, 2 h) and stored in a desiccator over phosphorus pentoxide (P_2O_5).

Characterization

Changes to TONc surface chemistry were examined by transmission FTIR on freeze-dried samples. Samples were mounted in KBr (Spectrograde Powder, International Crystal Labs, Garfield, NJ) at $\sim$1%

loading and examined in a Thermo Scientific Nicolet 8700 spectrometer. Spectra were obtained at room temperature under continuous purging with dry air and each spectrum was acquired from 32 scans at a resolution of 4 cm^{-1}. A separate background spectrum was collected and automatically subtracted from the raw spectrum for each specimen.

Conductometric titration (CT) was chosen to quantify carboxyl groups remaining after the modification treatments. CT was performed on dialyzed suspensions according to an earlier described procedure (Katz et al. 1984; Perez et al. 2003). Carboxyl concentrations were expressed as degree of oxidation (DO) according to Eq. 1 (Perez et al. 2003), with the denominator appropriately adjusted for our use of the free acid rather than the salt form.

$$DO = \frac{162 n_{COOH}}{w - 14 n_{COOH}} \quad (1)$$

where (162) is the molar mass of anhydroglucose unit (AGU), n_{COOH} is the moles of carboxylic acid in the sample (as obtained from CT data), w is the initial dry weight of the sample, and (14) represents the molecular weight difference between TONc (acid form) and unoxidized cellulose.

The degree of ODA substitution was calculated using nitrogen content data from the Kjeldahl technique. Kjeldahl tests were conducted on freeze-dried samples (~0.5 g) at Galbraith Laboratories Inc (GLI), Knoxville, TN according to GLI test protocol E7-1. Calculation of Degree of substitution (DS) was adapted from the method developed by (Vaca-Garcia et al. 2001) (online resource 1).

Advancing water contact angles were measured on film samples using the sessile drop technique. A dynamic CA analyzer (FTA200) was used to measure CAs of water sessile drops (~20 μL) on film samples. The samples were mounted on double-sided tapes attached to glass slides. Four hundred advancing CA images were acquired at a rate of 33 images per second, beginning at the instant the drop contacted the surface (0 s). The sequentially acquired CAs were subsequently plotted as a function of time.

Appearance of flow birefringence (Heux et al. 2000; Araki et al. 2001; van den Berg et al. 2007) was used as a qualitative measure of the ability of the modified TONc to disperse in organic solvents. Toluene ($\varepsilon = 2.38$), tetrahydrofuran (THF, $\varepsilon = 7.52$), and isopropyl alcohol (IPA, $\varepsilon = 20.2$) were chosen as low, intermediate, and high polarity organic solvents respectively. Suspensions (1 wt%) were prepared from freeze-dried samples, sonicated for 5 min, and photographed between crossed polarizers after gentle shaking. Suspension stabilities over the long term were also assessed by visual observation.

Crystalline properties were measured by wide angle X-ray diffraction (XRD) spectroscopy (Ni-filtered CuKα radiation ($\lambda = 1.54$ Å), 40 kv/40 mA) on a Bruker AXS D8 (Discover) X-ray diffractometer. Discs (7.5 mm wide) were punched out of films and stacked to thicknesses of ~800 μm (4 layers). Diffraction profiles were acquired in the 2θ range of 10–40° at 0.01° s^{-1}.

Thermal decomposition behaviors were studied on a Q500 thermogravimetric analyzer (TA Instruments). Freeze-dried samples (10–12 mg) were heat-scanned at 10 °C min^{-1} in dry air from room temperature to 600 °C. The high-resolution (Hi-Res™) dynamic heating rate mode (Salin and Seferis 1993) was used at resolution and sensitivity settings of 4 and 1 respectively.

Results and discussion

Octadecylamine coupling to TONc surfaces

FTIR confirms the presence of carboxylic acid (1,729 cm^{-1}, asymmetric C=O stretching) (Araki et al. 2001; Habibi et al. 2006; Saito et al. 2006a; Follain et al. 2008) in addition to characteristic native cellulose peaks in the spectrum of the TONc control (Fig. 3a). Following surface modification treatments, spectra of both ICmplx (Fig. 3b) and Amd (Fig. 3c) are characterized by bands common to TONc and ODA (Fig. 3a, d), indicating that both treatments were successful in attaching ODA to TONc surfaces. Also, with the disappearance of the C=O stretching (1,729 cm^{-1}) peak from the spectra of the modified samples, there appears to be complete substitution of TONc surface carboxyl groups by ODA molecules. In agreement with previous reports (Bulpitt and Aeschlimann 1999; Araki et al. 2001; Zhu et al. 2001; Follain et al. 2008), clear evidence of amide bonding, namely amide I (C=O stretching, 1,645 cm^{-1}), amide II (combined N–H deformation and C–N stretching, 1,549 cm^{-1}) and the N–H stretching (3,299 cm^{-1}) band of solid state secondary amides (Clothup et al.

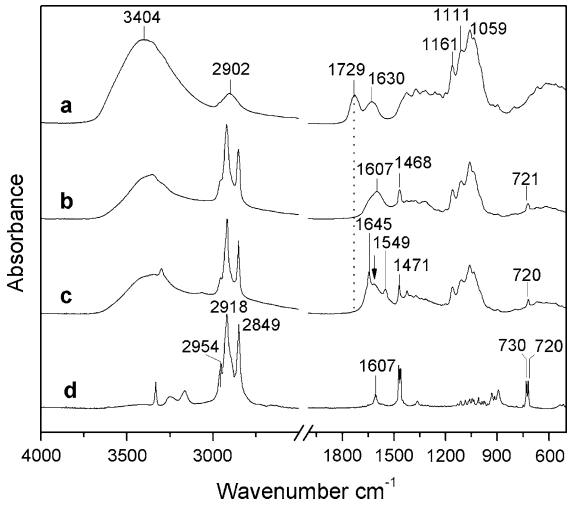

Fig. 3 FTIR spectra of (*a*) TONc control, (*b*) ICmplx (*c*) Amd, and (*d*) ODA. *Dotted line* marks the peak of the carbonyl stretching vibration in TONc, which is absent from the spectra of the ODA-modified samples. *Arrowed* 1,607 cm^{-1} peak indicates the possible presence of ionic complexes in Amd

1990) were observed in the spectrum of Amd (Fig. 3c). As can be expected in the absence of coupling agents, amide bonds are clearly absent from the spectrum of ICmplx; rather, a broad band appears with a peak at 1,607 cm^{-1} (Fig. 3b), which is characteristic of the asymmetric C=O stretching vibration of the COO^- group (1,550–1,610 cm^{-1}) (Williams and Fleming 1980; Clothup et al. 1990; Socrates 2001) generated from ion exchange between carboxylic protons and octadecylammonium cations (schematic depiction in Fig. 2). This peak also appears to be present in the spectrum of Amd (arrowed), overlapping with the amide I and amide II bands, and suggesting likely ionic complexation between ODA molecules and TONc carboxyl groups that failed to undergo amidation reaction. Consumption, by ionic complexation, of residual surface carboxyl groups that escaped covalent coupling may also explain the absence of any residual carbonyl peaks in the Amd spectrum. In the ICmplx spectrum (Fig. 3b), a weaker symmetric C=O stretching vibration of the COO^- group was expected in the 1,410–1,430 cm^{-1} region but it appears to have been obscured by the strong –CH deformation vibration located at 1,468 cm^{-1}.

Another interesting finding is the resistance of ICmplx to regeneration of –COOH groups following exposure to acidic media. The nanocellulose recovery process following modification reactions included HCl washing at pH 1.3–1.4, which was expected to regenerate –COOH groups from the octadecylammonium carboxylate complexes. As FTIR results have shown, regeneration of –COOH did not occur. In a related study, Saito and Isogai reported the metal ion-dependent stability of metal ion carboxylate salts prepared by ion exchange between the sodium salt of TEMPO-oxidized cellulose and a variety of metal ions (Pb^{2+}, La^{3+}, Al^{3+}, Ca^{2+}, Ba^{2+}, Ni^{2+}, Co^{2+}, Cd^{2+}, Sr^{2+}, Mn^{2+}, Ca^{2+}, and Mg^{2+}) (Saito and Isogai 2005) Resistance of the various metal carboxylate salts to dissociation was examined by exposing the ion-exchanged oxidized fibers to nitric acid (HNO_3) solution (pH 1.7) and sodium nitrate ($NaNO_3$) solution (pH 7.0). Approximately 20% of Pb^{2+} and La^{3+} ions remained in their respective HNO_3–treated fibers compared to a near complete generation of free carboxylic acids in the fibers exchanged to the other metal ions. Also, substantially higher residual Pb^{2+} and La^{3+} concentrations remained in the $NaNO_3$–treated fibers relative to the HNO_3–treated samples. In the present study, a hydrophobic shielding effect is hypothesized. It is speculated that the alkyl tails of the attached octadecylammonium groups create a strongly hydrophobic environment in the immediate vicinity of modified nanofibrils, which resists dissociation in the low pH environment.

Degree of ODA substitution

Conductometric titration was used to obtain the amounts of carboxyl groups remaining after surface modification treatments, expressed as DO in Table 1. Representative CT plots of the modified TONc (Fig. 4b, c) show the absence of a weak acid neutralization region, which, in the control sample plot, is represented by the flat region (Fig. 4a)). With respect to the modified TONc, the absence of this

Table 1 Properties of control and ODA-modified TONc

Name	DO	DS	CA, deg
TONc control	0.262 (0.001)	–	36.3 (1.0)
Amd	0	0.267 (0.004)	108 (2.0)
ICmplx	0	0.289 (0.007)	118 (3.0)

DO degree of oxidation, *DS* degree of ODA substitution, and *CA* advancing water contact angle from sessile drop technique

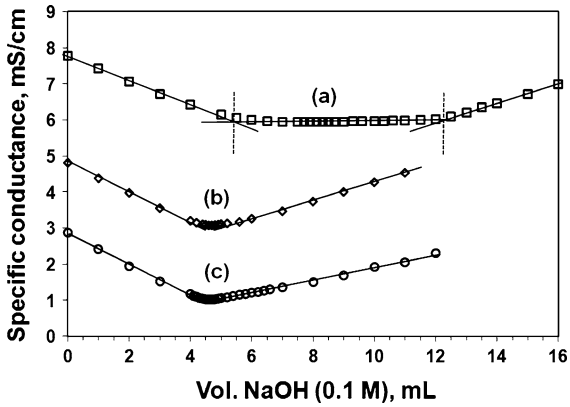

Fig. 4 Representative conductometric titration curves for (*a*) TONc control, (*b*) ICmplx, and (*c*) Amd. The flat region of curve (*a*) (between *dotted lines*) represents weak carboxylic acid neutralization, from which carboxyl content of TONc is determined. No carboxylic acid neutralization regions are observed in curves (*b*) and (*c*), indicating complete consumption of available carboxylic acid groups during the surface modification processes

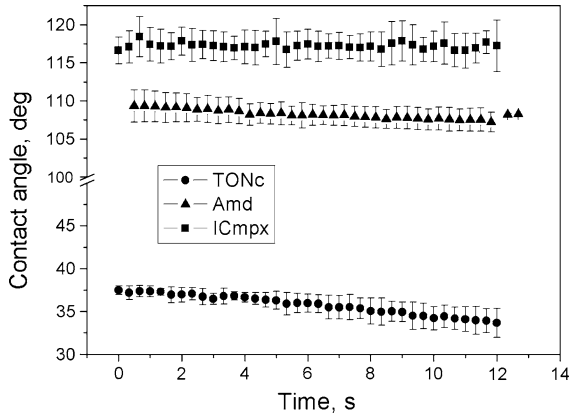

Fig. 5 Time-dependent advancing water contact angles on film samples. *Error bars* represent ± 1 standard deviations from three replications

region indicates an absence of COO^- groups (i.e. DO = 0, Table 1) and confirms complete consumption of available carboxyl groups during both amidation and ionic complexation treatments. This result is also consistent with the observed absence of C=O peaks in the FTIR spectra of Amd and ICmplx (Fig. 3).

Kjeldahl N analysis was utilized as an indirect method to evaluate the degrees of ODA substitution from the surface modification treatments (Table 1). From Table 1, the amount of ODA in Amd (DS) is statistically equivalent to the amount of starting carboxyl (DO of control), which provides additional evidence for the complete carboxyl to ODA substitution indicated by the FTIR and CT results. With respect to ICmplx, a slight excess of ODA relative to the starting TONc carboxyl content suggests a greater than one-to-one substitution of carboxyl groups by ODA molecules (DS of ICmplx vs. DO of control). This slightly greater ODA loading in ICmplx is also manifested, qualitatively, in the CA and TGA results discussed below.

Surface polarity

CA analysis

Time-dependent advancing CAs of water droplets on film samples (Fig. 5) illustrate changes to TONc surface polarity after the surface modification treatments. A mean CA of 36.3 ± 1.0° was calculated from the data of the TONc control, confirming its hydrophilic character. Mean CAs increase to 108 ± 2.0 and 118 ± 3.0 upon amidation and ionic complexation respectively. These changes mark a transformation of TONc surfaces to hydrophobic character as a result of ODA substitution. The data also indicate a slightly greater hydrophobicity of ICmplx surface, which is consistent with the evidence of a slightly higher ODA concentration from elemental analysis.

Dispersibility in organic solvents

Appearances of flow birefringence and chiral-nematic self ordering are routinely used as qualitative evidence for the dispersion of surface-modified nanocelluloses in organic media (Heux et al. 2000; Araki et al. 2001; Gousse et al. 2002; Yuan et al. 2006; Petersson et al. 2009; Zhou et al. 2009). In Fig. 6a, an aqueous suspension of TONc control depicts strong birefringence, in agreement with past reports (Habibi et al. 2006; Saito et al. 2006a, 2007). The freeze-dried Amd and ICmplx nanofibrils on the other hand, could not be dispersed in water. They merely floated on or remained distinctly separated from water even after vigorous shaking. They, however, could be readily dispersed and did display birefringence in all three organic solvents (Fig. 6b–f) of widely varying polarities. The wide ranging dispersibilities may be related to the fact that both hydrophobic (ODA pendants) and

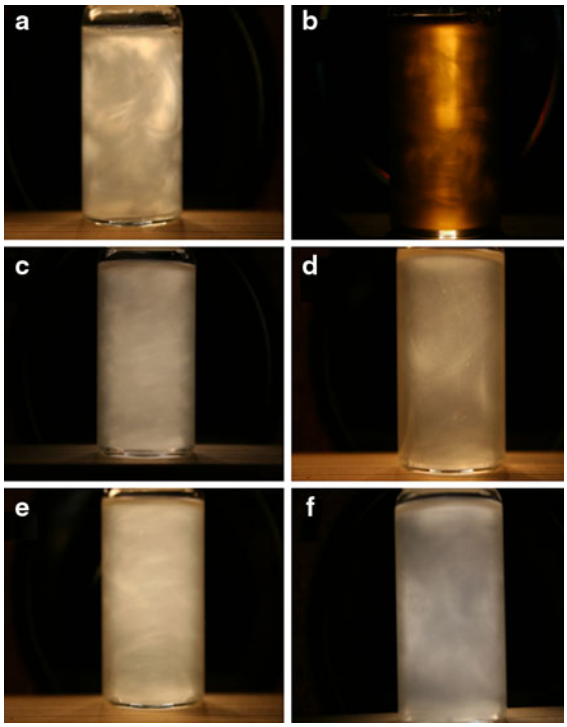

Fig. 6 Birefringent dispersions of **a** TONc in water, **b** Amd in toluene, **c** Amd in THF, **d** Amd in IPA, **e** ICmplx in THF, and **f** ICmplx in IPA. Nanocellulose concentrations in (a) = 0.125 wt% and (b–f) = 0.5 wt%. Pictures taken ~5 s after vigorous shaking of the vials

hydrophilic (uncoupled secondary –OH at C2 and C3 positions of AGUs) groups are present on the TONc surfaces. Also, the ability of ICmplx to disperse as efficiently as the covalently coupled Amd is interesting, in that it illustrates the reliability of a simple ion exchange rather than an elaborate covalent coupling technique to achieve significant surface hydrophobization of nanocelluloses. Recently, Isogai and coworkers (Isogai et al. 2011) reported an elegant approach to effectively disperse TONc, without further surface modification, in organic solvents. They performed a sequential solvent exchange followed by evaporation of the undesirable solvent leaving the TONc in the solvent of interest. With a final sonication step, they achieved excellent TONc dispersion in *N*,*N*-dimethylformamide, *N*,*N*-dimethylacetamide, dimethylsulfoxide, 1,3-dimethyl-2-imidazolidinone, and 1-methyl-2-pyrrolidinone. The approach was successful in achieving stable birefringent dispersions of the free acid form of TONc in four of the five solvents tested whereas the sodium form of TONc could only be dispersed in DMSO. The mechanisms for dispersibility were proposed as interfibrillar electrostatic repulsion and/or osmotic effects. The authors also indicated solvent dielectric constant and viscosity as significant contributors to fibril dispersibility. One distinguishing difference between their approach and the current study is their inability to achieve birefringence in lower boiling organic solvents such as THF and IPA.

In addition to flow birefringence, long-term stability of nanocellulose suspensions is highly desirable, especially as it relates to solvent casting of nanocomposites. Based on the observed birefringence behavior, suspensions of the ODA-modified TONc were expected to remain stable over time as other studies involving both adsorption (Heux et al. 2000; Zhou et al. 2009) and covalent coupling (Gousse et al. 2002) to nanocellulose surfaces have demonstrated. Rather surprisingly, however, the nanofibrils from the present study began to settle within 5 min after agitation, and in matter of several hours, phase separation was clearly observed. The rate of settling was also observed to be different between the two modified samples, being higher for Amd (Fig. 7). For example, within 3 days, flocculation in THF was far more advanced in Amd than ICmplx (Fig. 7a) although the extent of flocculation was equivalent for both materials after 7 days at rest (Fig. 7b). The difference in initial rates of flocculation is consistent with the noted, slightly higher ODA content of ICmplx as determined from elemental analysis. No effort was made to ascertain the causes of nanofibril aggregation, however, it can be speculated that unoxidized surface hydroxyl groups remaining at the C2 and C3 positions of the modified nanocelluloses may be involved in interfibrillar hydrogen bonding that overcomes both fibril-solvent interactions and the weaker non-polar interactions between attached ODA groups and the organic solvent medium.

Crystallinity

TEMPO-mediated oxidation has been shown to affect only the hydroxyl groups in the amorphous regions and at the surfaces of cellulose I crystallites (Saito and Isogai 2004; Habibi et al. 2008; Okita et al. 2009; Saito et al. 2009), leaving the core crystalline domains unchanged. The X-ray diffraction profiles of both the TONc control and ODA-modified TONc (Fig. 8) are representative of wood-derived cellulose

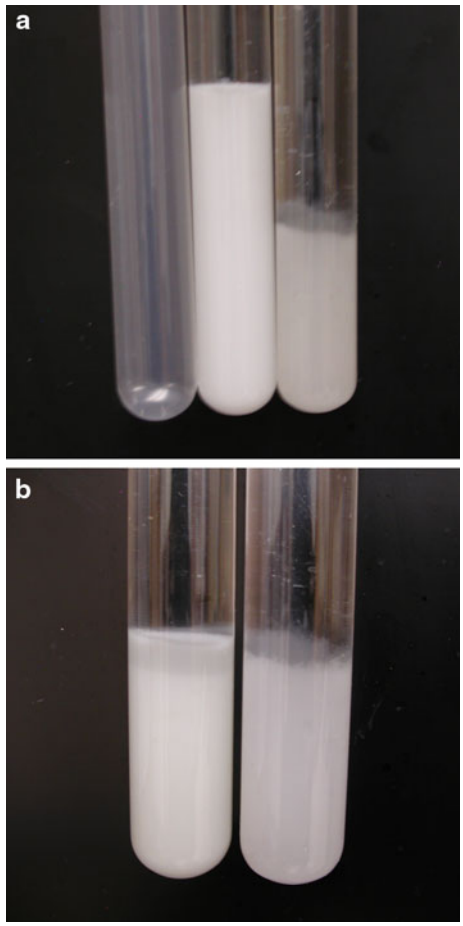

Fig. 7 **a** Three-day old suspensions of TONc in water (*left*), ICmplx (*middle*), and Amd (*right*) in THF. **b** ICmplx (*left*) and Amd (*right*) suspensions in THF after 7 days

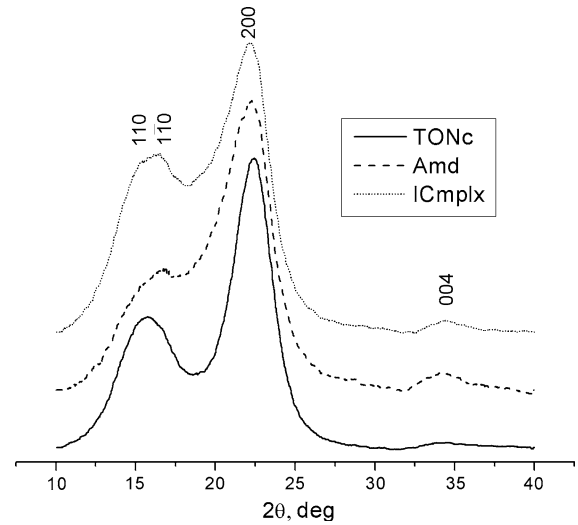

Fig. 8 X-ray diffraction profiles of film samples (thicknesses ~800 μm) labeled with corresponding reflection planes

(Saito et al. 2009; Okita et al. 2010), indicating that the crystalline structure of cellulose is unaltered by the surface modification treatments. In addition, no new reflections are evident in the Amd and ICmplx curves, which suggests that the attached ODA groups might exist in non-crystalline form. This observation is borne out by differences between the FTIR spectra of neat ODA and the modified TONc. In the neat ODA spectrum (Fig. 3d), the 720 and ~1,470 cm^{-1} ($–CH_2$ rocking and –CH bending vibrations respectively) are split as a result of crystalline orientation (Clothup et al. 1990). These absorbances, however, appear as single peaks in the Amd and ICmplx spectra (Fig. 3b, c), which is evidence of the absence of crystallinity among the ODA alkyl chains.

Thermal degradation properties

Weight loss and derivative of weight loss versus temperature plots (Fig. 9) for TONc and its modified derivatives reveal multiple degradation events. TEMPO-mediated oxidation significantly decreases the thermal stability of native cellulose (Fukuzumi et al. 2009; Johnson et al. 2009; Fukuzumi et al. 2010) due to decarbonation of the formed anhydroglucuronic acid groups (Fukuzumi et al. 2010). In Fig. 9b, the main decomposition event of TONc is resolved into two peaks, which likely represents decomposition of TONc surface and core fractions. With ODA substitution (Amd and ICmplx in Fig. 9b), the peak of the main decomposition event is shifted to slightly higher temperatures, indicating a slight improvement in thermal stability relative to the TONc control. Also, the peak intensity of the ICmplx decomposition step is higher than that of Amd, possibly due to the different thermal resistances of the ionic versus covalent bond types associated with the two treatments, and, perhaps, the slightly greater ODA content in ICmplx. Also present in the modified TONc thermograms are three weight loss events preceding the main decomposition step (Fig. 9b). The first (below 100 °C) may be attributed to loss of some bound volatile material, probably bound solvent. With respect to the subsequent two events (peaks at 185 and ~220 °C), a possible volatilization of

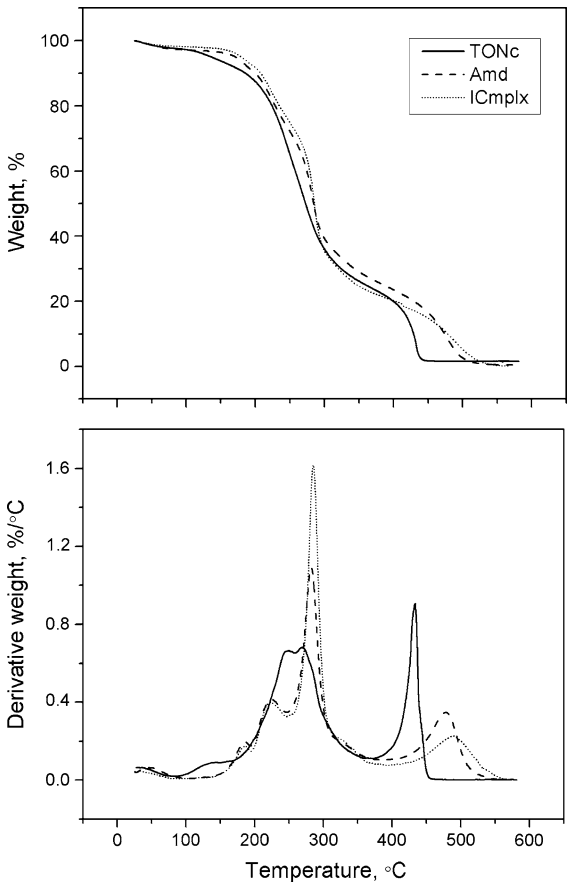

Fig. 9 TGA weight loss and derivative weight loss plots as a function of temperature

attached ODA groups was hypothesized. In an attempt to verify this, Amd and ICmplx samples were heated to 250 °C (upper limit of the higher thermal degradation event), for 1 h, and the recovered residue was examined in FTIR. The resulting spectra (online resource 2) showed clear evidence of continued ODA presence but substantial changes to the 800–1,800 cm^{-1} region. Future work, with the aid of a TG-FTIR analyzer, could make possible the identification of these decomposition events. The higher temperature events (peaks > 400 °C) are attributed to ignition of the left-over carbonaceous residue from the main decomposition event,[1] and have been described as the region of "glowing combustion" due to the self-sustaining exothermic nature of the reaction (Aggarwal and Dollimore 1997). Consistent with the shifts to slightly higher temperatures in the main decomposition event, char decomposition of both Amd and ICmplx are also shifted to higher temperatures, indicating an overall improvement in TONc thermal stability as a result of ODA coupling.

[1] Reported for the combustion of cationically-modified microcrystalline cellulose and corn starch in air atmosphere (Aggarwal and Dollimore 1997).

Conclusions

It is concluded that with the aid of a co-solvent system, both electrostatic and covalent attachment of ODA to TONc surfaces can be easily achieved, through the use of ionic complexation and carbodiimide-mediated amidation respectively. ICmplx is surprisingly resistant to dissociation under low pH conditions, which may have resulted from the creation, by attached ODA groups, of a strongly hydrophobic environment in the immediate vicinity of the modified nanofibrils. By using a co-solvent system as the reaction medium, available TONc carboxyl groups are shown to be completely substituted by ODA molecules leading to remarkably low surface polarities and excellent organic solvent dispersions of the modified nanofibrils. Under the possible influence of interfibrillar hydrogen bonding between the C2 and C3 –OH groups on TONc surfaces, long-term stability of the organic solvent dispersions of the ODA-modified TONc cannot be achieved using the present treatment conditions. The cellulose I crystalline structure of TONc is preserved after coupling to ODA as revealed by similarities in shape of XRD diagrams. The thermal stability of TONc is slightly improved by coupling to ODA but the product of ionic complexation decomposes with greater intensity, possibly due to the relatively less energetic electrostatic interactions involved and its slightly higher ODA content.

Acknowledgments This study was carried out with the financial support of the Sustainable Engineered Materials Institute (SEMI), Virginia Tech College of Natural Resources and Environment in Blacksburg, Virginia.

References

Aggarwal P, Dollimore D (1997) The combustion of starch, cellulose and cationically modified products of these compounds investigated using thermal analysis. Thermochim Acta 291:65–72

Araki J, Wada M, Kuga S (2001) Steric stabilization of a cellulose microcrystal suspension by poly(ethylene glycol) grafting. Langmuir 17:21–27

Azzam F, Heux L, Putaux JL, Jean B (2010) Preparation by grafting onto, characterization, and properties of thermally responsive polymer-decorated cellulose nanocrystals. Biomacromolecules 11:3652–3659

Bulpitt P, Aeschlimann D (1999) New strategy for chemical modification of hyaluronic acid: preparation of functionalized derivatives and their use in the formation of novel biocompatible hydrogels. J Biomed Mater Res 47:152–169

Clothup NB, Daly LH, Wiberley SE (1990) Introduction to infrared and Raman spectroscopy. Academic Press Inc, San Diego

Follain N, Montanari S, Jeacomine I, Gambarelli S, Vignon MR (2008) Coupling of amines with polyglucuronic acid: evidence for amide bond formation. Carbohydr Polym 74:333–343

Follain N, Marais MF, Montanari S, Vignon MR (2010) Coupling onto surface carboxylated cellulose nanocrystals. Polymer 51:5332–5344

Fukuzumi H, Saito T, Wata T, Kumamoto Y, Isogai A (2009) Transparent and high gas barrier films of cellulose nanofibers prepared by TEMPO-mediated oxidation. Biomacromolecules 10:162–165

Fukuzumi H, Saito T, Okita Y, Isogai A (2010) Thermal stabilization of TEMPO-oxidized cellulose. Polym Degrad Stab 95:1502–1508

Gousse C, Chanzy H, Excoffier G, Soubeyrand L, Fleury E (2002) Stable suspensions of partially silylated cellulose whiskers dispersed in organic solvents. Polymer 43: 2645–2651

Habibi Y, Chanzy H, Vignon MR (2006) TEMPO-mediated surface oxidation of cellulose whiskers. Cellulose 13:679–687

Habibi Y, Goffin AL, Schiltz N, Duquesne E, Dubois P, Dufresne A (2008) Bionanocomposites based on poly(epsilon-caprolactone)-grafted cellulose nanocrystals by ring-opening polymerization. J Mater Chem 18:5002–5010

Heux L, Chauve G, Bonini C (2000) Nonflocculating and chiral-nematic self-ordering of cellulose microcrystals suspensions in nonpolar solvents. Langmuir 16:8210–8212

Isogai A, Kado H, Goi Y (2010a) Cosmetics compositions containing oxidized cellulose fibers and functional components. Daiichi Kogyo Seiyaku Co., Ltd., Japan. Application: JP, 19 pp

Isogai A, Kado H, Goi Y (2010b) Gel compositions containing oxidized cellulose fibers with good resistance to salts and ionic surfactants. Daiichi Kogyo Seiyaku Co., Ltd., Japan. Application: JP, 43 pp

Isogai A, Kado H, Goi Y (2010c) Spray compositions containing oxidized cellulose fibers as thickeners, and sprayers therefor. Daiichi Kogyo Seiyaku Co., Ltd., Japan. Application: JP, 25 pp

Isogai A, Okita Y, Fujisawa S, Saito T (2011) TEMPO-oxidized cellulose nanofibrils dispersed in organic solvents. Biomacromolecules 12:518–522

Johnson RK, Zink-Sharp A, Renneckar SH, Glasser WG (2009) A new bio-based nanocomposite: fibrillated TEMPO-oxidized celluloses in hydroxypropyl cellulose matrix. Cellulose 16:227–238

Kato T, Isogai A, Saito T, Oaki Y, Nishimura T (2010) Composite material, functional material, process for producing composite material, and process for producing composite-material thin film. Chemical Indexing Equivalent to 152:264550 (WO) pp. Tokyo University, Japan. Application: JP, 38 pp

Katz S, Beatson RP, Scallan AM (1984) The determination of strong and weak acidic groups in sulfite pulps. Svensk Papperstidning 87:R48–R53

Lasseuguette E (2008) Grafting onto microfibrils of native cellulose. Cellulose 15:571–580

Li Z, Renneckar S, Barone JR (2010) Nanocomposites prepared by in situ enzymatic polymerization of phenol with TEMPO-oxidized nanocellulose. Cellulose 17:57–68

Mukai K, Kumamoto Y, Isogai A, Meiwa Z, Maezawa T, Ugajin T (2010) Gas-barrier material, gas-barrier molded article, and method for producing the gas-barrier molded article. Kao Corporation, Japan. Application: WO, 108 pp

Okita Y, Saito T, Isogai A (2009) TEMPO-mediated oxidation of softwood thermomechanical pulp. Holzforschung 63:529–535

Okita Y, Saito T, Isogai A (2010) Entire surface oxidation of various cellulose microfibrils by TEMPO-mediated oxidation. Biomacromolecules 11:1696–1700

Perez DD, Montanari S, Vignon MR (2003) TEMPO-mediated oxidation of cellulose III. Biomacromolecules 4:1417–1425

Petersson L, Mathew AP, Oksman K (2009) Dispersion and properties of cellulose nanowhiskers and layered silicates in cellulose acetate butyrate nanocomposites. J Appl Polym Sci 112:2001–2009

Saito T, Isogai A (2004) TEMPO-mediated oxidation of native cellulose. The effect of oxidation conditions on chemical and crystal structures of the water-insoluble fractions. Biomacromolecules 5:1983–1989

Saito T, Isogai A (2005) Ion-exchange behavior of carboxylate groups in fibrous cellulose oxidized by the TEMPO-mediated system. Carbohydr Polym 61:183–190

Saito T, Shibata I, Isogai A, Suguri N, Sumikawa N (2005) Distribution of carboxylate groups introduced into cotton linters by the TEMPO-mediated oxidation. Carbohydr Polym 61:414–419

Saito T, Nishiyama Y, Putaux JL, Vignon M, Isogai A (2006a) Homogeneous suspensions of individualized microfibrils from TEMPO-catalyzed oxidation of native cellulose. Biomacromolecules 7:1687–1691

Saito T, Okita Y, Nge TT, Sugiyama J, Isogai A (2006b) TEMPO-mediated oxidation of native cellulose: microscopic analysis of fibrous fractions in the oxidized products. Carbohydr Polym 65:435–440

Saito T, Kimura S, Nishiyama Y, Isogai A (2007) Cellulose nanofibers prepared by TEMPO-mediated oxidation of native cellulose. Biomacromolecules 8:2485–2491

Saito T, Hirota M, Tamura N, Kimura S, Fukuzumi H, Heux L, Isogai A (2009) Individualization of nano-sized plant cellulose fibrils by direct surface carboxylation using TEMPO catalyst under neutral conditions. Biomacromolecules 10:1992–1996

Salin IM, Seferis JC (1993) Kinetic-analysis of high-resolution TGA variable heating rate data. J Appl Polym Sci 47:847–856

Socrates G (2001) Infrared and Raman characteristic group frequencies. Wiley, Chichester

Suzuki A, Miyawaki S, Katsukawa S, Abe H, Iijima Y, Isogai A (2009) Cellulose nanofiber-containing base paper for processing paper. Nippon Paper Industries Co., Ltd., Japan. Application: JP, 10 pp

Vaca-Garcia C, Borredon ME, Gaseta A (2001) Determination of the degree of substitution (DS) of mixed cellulose esters by elemental analysis. Cellulose 8:225–231

van den Berg O, Capadona JR, Weder C (2007) Preparation of homogeneous dispersions of tunicate cellulose whiskers in organic solvents. Biomacromolecules 8:1353–1357

Williams DH, Fleming I (1980) Spectroscopic methods in organic Chemistr. McGraw-Hill Book Company (UK) Ltd., London

Yuan HH, Nishiyama Y, Wada M, Kuga S (2006) Surface acylation of cellulose whiskers by drying aqueous emulsion. Biomacromolecules 7:696–700

Zhou Q, Brumer H, Teeri TT (2009) Self-organization of cellulose nanocrystals adsorbed with xyloglucan oligosaccharide-poly(ethylene glycol)-polystyrene triblock copolymer. Macromolecules 42:5430–5432

Zhu LH, Kumar V, Banker GS (2001) Examination of oxidized cellulose as a macromolecular prodrug carrier: preparation and characterization of an oxidized cellulose-phenylpropanolamine conjugate. Int J Pharm 223:35–47